Linear PM Generator System for Wave Energy Conversion in the AWS

Henk Polinder, *Member, IEEE*, Michiel E. C. Damen, and Fred Gardner

***Abstract*—The Archimedes Wave Swing is a system that converts ocean wave energy into electric energy. A pilot plant of this system has been built. The generator system consists of a permanent-magnet linear synchronous generator with a current source inverter (CSI). The correlation between the measured and the calculated parameters of the designed generator is reasonable. The annual energy yield of the pilot plant is calculated from the wave distribution as 1.64 GWh. Using a voltage source inverter instead of a CSI improves the power factor, the current waveforms, the efficiency and the generator force, so that the annual energy yield increases with 18%.**

***Index Terms*—Converters, energy yield, linear synchronous generators, permanent-magnet generators, wave energy.**

I. Introduction

SIGNIFICANT factors which have stimulated the use of renewable energy are energy cost, energy independence and mainly environmental protection. Therefore, great efforts are made in the fields of wind energy, solar energy, hydro power, and so on. Ocean wave energy is a renewable energy source with a huge potential, but further from commercial viability. Different wave energy conversion systems have been proposed. The following concepts may be distinguished [1]–[7].

1) Buoyant moored devices have a floater that is moved by the waves. Energy is extracted from this motion. The motion may be up and down or around an axis.
2) Hinged contour devices consist of different floaters that move with respect to each other when waves pass. From this motion, energy is extracted, mostly with hydraulic pumps.
3) Oscillating water columns are chambers where the water level rises and falls with the waves. The air coming into and going out of this chamber drives a wells turbine connected to a generator.
4) Overtopping devices are water reservoirs which are filled by waves via some kind of wave concentrator which increases the wave height. The water leaves the reservoir via a water turbine driving a generator.

This paper is about the Archimedes Wave Swing (AWS). The idea behind this system originates from 1993, when F. Gardner and H. van Breugel started to work out their ideas on wave energy conversion [8].

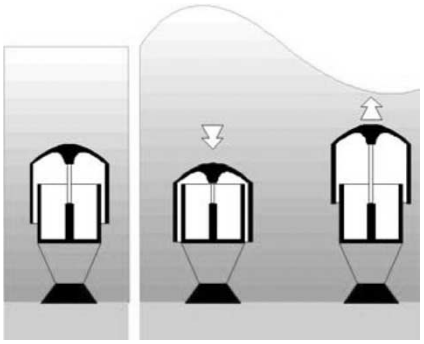

Fig. 1. Sketch of the AWS illustrating the operation principle.

Fig. 1 illustrates the principle of operation. Basically, the AWS is a cylindrical air-filled chamber. The waves move the lid of this chamber, called the floater, in vertical direction with respect to the bottom part, which is fixed to the sea-bottom. When a wave is above the AWS, the AWS volume is reduced by the high water pressure. When a wave trough is above the AWS, the volume increases because of the air pressure inside the AWS. From this linear motion, energy can be extracted and converted into electrical energy.

The AWS is a unique wave energy conversion system because it is completely submerged. This is important, because this makes the system less vulnerable in storms. Besides, it is not visible, so that the public acceptance is not such a problem as for, for example, wind farms.

To prove the principle of operation behind this idea, a few small models have been developed (scale 1:20 and 1:50 to the final system) [9]. These models showed that the system worked and validated the models predicting the hydrodynamic forces on and the hydrodynamic damping of the floater.

As a next step, a pilot plant of the AWS has been built at the Portugese coast. The main objective of this pilot plant is to prove that the complete system works and can survive. Until now, the system has not been submerged. Therefore, full scale experimental results are not yet available.

Fig. 2 depicts a photograph of the pilot plant. The maximum peak power is 2 MW; the maximum average power is 1 MW. The centre part contains the floater with a diameter of 9 m. The rated stroke is 7 m and the rated velocity is 2.2 m/s.

It is possible to convert the linear floater motion into rotating motion and use a rotating generator. However, it appears to be extremely difficult to build a robust, maintenance-free gear. Therefore, a linear generator is used.

Manuscript received July 3, 2003. Paper no. TEC-00022-2003.

H. Polinder is with the Electrical Power Processing Group, Delft University of Technology, Delft NL 2628 CD, The Netherlands (e-mail: h.polinder@ewi.tudelft.nl).

M. E. C. Damen and F. Gardner are with Teamwork Technology BV, Zijdewind 1736 KB, The Netherlands. M. E. C. Damen is also with Technical Highschool Rijswijk, Rijswijk 2288 GK, The Netherlands (e-mail: dam@thrijswijk.nl; fred.gardner@teamwork.nl).

Digital Object Identifier 10.1109/TEC.2004.827717

Fig. 2. Photo of the AWS pilot plant before submerging.

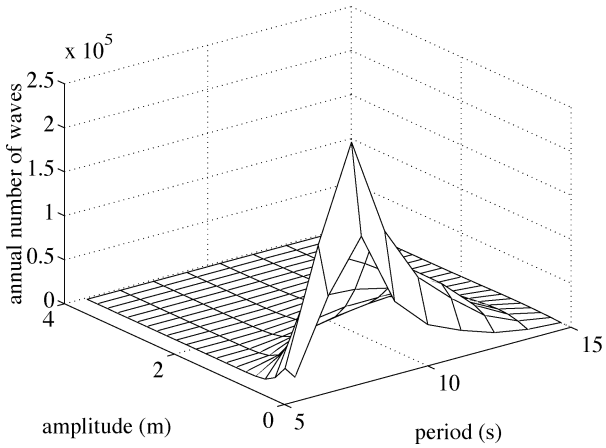

Fig. 3. Annual number of waves energy yield as a function of wave amplitude and wave period.

It is nearly impossible to make the generator large enough to take all possible forces generated by waves. Therefore, the AWS also has water dampers that can make very high forces. This also implies that the generator can be designed as a compromise between energy yield and cost.

The generator terminals are connected to a 6-km-long cable, which brings the power to the shore. A current source inverter (CSI) on the shore is used for the utility grid connection.

The objective of this paper is to describe the main characteristics of the AWS generator system and to motivate some of the design choices. Therefore, the paper starts with the calculation of the expected annual energy yield based on the principle of operation. Next, the generator design and performance are discussed together with the results of some generator tests. Subsequently, the use of a voltage source inverter (VSI) and a CSI are compared. The paper ends with some conclusions.

II. Energy Yield Calculations

A. Theoretical Derivations

To be able to calculate energy yield, a good understanding of the physical behavior of the AWS is necessary. Therefore, we start with the equation describing the vertical floater position y, as follows:

$$(M_{fl}+M_{ad})\frac{\mathrm{d}^2y}{\mathrm{d}t^2}+(\beta_h+\beta_g)\frac{\mathrm{d}y}{\mathrm{d}t}+C_{AWS}y=F_w \qquad (1)$$

where

- M_{fl} floater mass;
- M_{ad} an added mass representing the water above the floater that has to be accelerated;
- β_h hydrodynamic damping coefficient of the AWS;
- β_g the damping coefficient provided by the generator;
- C_{AWS} the spring constant of the AWS;
- F_w wave diffraction force on the floater.

Both the hydrodynamic damping coefficient β_h and the diffraction force F_w have been calculated as a function of wave amplitude and the wave period [8], [9]. For a scale models, these calculations have been successfully validated [8] by measuring the wave diffraction force F_w for a fixed floater position and by measuring the floater position as a function of time for free floater oscillation, from which the hydrodynamic damping β_h can be determined.

The maximum amount of energy is taken by the generator system when the system is in resonance

$$(M_{fl}+M_{ad})\frac{\mathrm{d}^2y}{\mathrm{d}t^2}+C_{AWS}y=0 \qquad (2)$$

and the hydrodynamic damping is equal to the damping provided by the generator $\beta_g=\beta_h$.

When there is resonance, the wave force acting on the floater, the floater position and the floater speed are all sinusoidal functions of time with the period of the waves. The floater stroke may be much higher than the wave height. Because the generator has to provide a damping, the generator force is also a sinusoidal function of time.

To bring the AWS in resonance with waves of different frequency, the spring constant C_{AWS} can be changed by changing the air pressure and volume inside the AWS.

Using these equations for a wave with a given amplitude and period, the energy that can be taken from this wave can be calculated as

$$E_w=\int_0^{T_w}P_w\mathrm{d}t=\int_0^{T_w}\beta_h\left(\frac{\mathrm{d}y}{\mathrm{d}t}\right)^2\mathrm{d}t=\int_0^{T_w}\frac{F_w^2}{4\beta_h}\mathrm{d}t=T_w\frac{F_{w\,\max}^2}{8\beta_h}. \qquad (3)$$

By counting the annual number of waves as a function of wave amplitude and period, the annual energy yield can be calculated. The number of waves as a function of wave amplitude and period for the location in Portugal is given in Fig. 3. Fig. 4 depicts the energy that can be taken from the waves in this way. From this figure, we conclude that increasing the wave period range or the wave amplitude range will hardly increase the energy yield. The total annual energy taken by the generator system is calculated as 8.55 GWh.

B. Practical Limitations

In reality, the annual energy taken by the generator system will be smaller for several reasons [10].

1) For many waves, applying this principle would lead to strokes and velocities that are much higher than possible

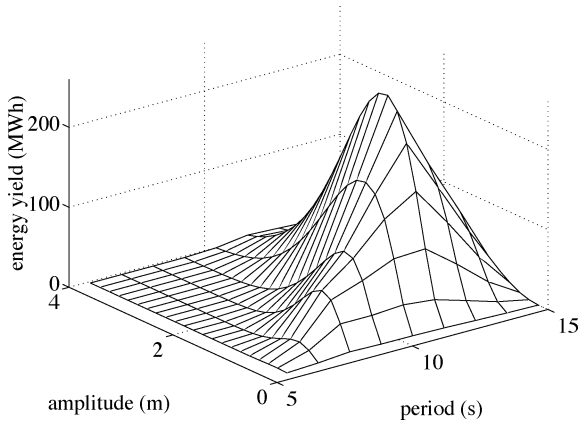

Fig. 4. Maximum annual energy yield that can be taken from the waves as a function of wave amplitude and wave period.

with the AWS. If this is the case, the generator force (the damping) is increased to reduce the stroke to 7 m and the velocity to 2.2 m/s. This reduces the annual energy taken by the generator system to 2.79 GWh. It can be concluded that increasing the stroke and the speed will increase the annual energy yield.

2) The force that can be made with the generator is limited. If the required force is larger, the water dampers are also used, which reduces the annual energy yield. If the generator force is limited to 659 kN (as is the case with a CSI), the annual energy taken by the generator system reduces to 2.41 GWh. If the generator force is limited to 933 kN (as is the case with a VSI), the annual energy taken by the generator system reduces to 2.63 GWh.
3) This calculation assumes that there is perfect resonance, which in reality is not the case because the wave period is continuously changing. However, simulations of the real floater motion show that the order of magnitude of the calculated energy yield is realistic.

III. Generator Design and Performance

A. Linear Permanent-Magnet Generator Design

A linear generator capable of making about 1 MN was not available. Therefore, a generator was designed and built.

A permanent-magnet linear synchronous generator (PMLSM) with magnets on the translator (the moving part) was chosen because:

- it has a rather high force density;
- it has a reasonable efficiency at low speeds;
- magnets are not that expensive anymore;
- there is no electrical contact to the translator.

Fig. 5 depicts a cross-section of the generator. Table I provides an idea about some important dimensions.

The attractive forces between stator and translator form a dangerous load for the bearings. To reduce the bearing load, the generator is double sided, as depicted in Fig. 5.

To reduce cost, the translator with the magnets is only three meters longer than the stator. Therefore, the overlap between stator and translator is complete when the force is maximum (in the central position) and the overlap is partial when the force is lower.

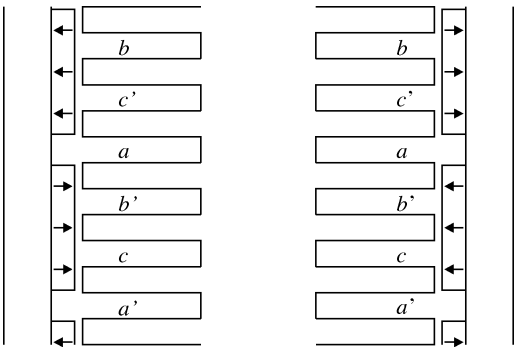

Fig. 5. Sketch of a section of a generator part.

TABLE I
Rough Generator Characteristics

length of the two double-sided stators	5 m
length of the four translators	8 m
width (stack length) of stators and translators	1 m
pole pitch	0.1 m
maximum RMS value of the current density	4 A/mm^2

The machine is designed so that the stator leakage inductance is larger than the main inductance to prevent magnet demagnetization in case of an accidental short circuit [11]. For the same reason, the number of slots per pole per phase is chosen one. Even at high loads, the flux density in the stator iron is kept low enough to prevent heavy saturation, as shown in [12].

Patterson *et al.* [13] propose a linear PM machine with a comparable force for a completely different application with very high speeds, namely for an aircraft launch system. They also use a double-sided construction with magnets on the translator, but because of different requirements, their translator is short and positioned between two stator sides.

The machine parameters are calculated in conventional ways [14]. The calculation of the no-load flux linkage is shown here, because it is compared with measurements later in the paper

$$\hat{\lambda}_{pm} = k_w N_s l_s \tau_p \frac{2}{\pi} \hat{B}_{gm} \tag{4}$$

where

k_w winding factor;
N_s number of turns of the winding;
τ_p pole pitch;
l_s stack length of the machine perpendicular to the plane of the drawing of Fig. 5;
$\hat{B}_{\rm gm}$ fundamental space harmonic of the magnetic flux density in the air gap due to the magnets

$$\hat{B}_{\rm gm} = \frac{l_m}{\mu_{\rm rm} g_{eff}} B_{\rm rm} \frac{4}{\pi} \sin\left(\frac{\pi b_b}{2\tau_p}\right) \tag{5}$$

where

l_m magnet length parallel to the magnetization;
$\mu_{\rm rm}$ relative recoil permeability of the magnets;

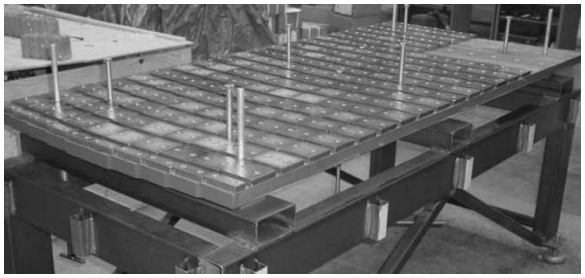

Fig. 6. Photo of a translator segment with magnets in production.

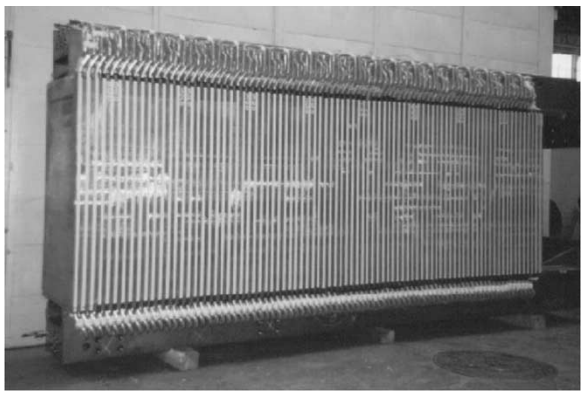

Fig. 7. Photo of a stator segment with coils.

$B_{\rm rm}$ remanent flux density of the magnets;
b_p width of the magnet;
$g_{\rm eff}$ effective air gap of the machine, given by

$$g_{eff} = \left(g + \frac{l_m}{\mu_{\rm rm}} \right) k_C \tag{6}$$

where
g mechanical air gap;
k_C Carter factor [14].

Fig. 6 depicts a photo of a translator segment with magnets on back iron. The magnets are skewed to reduce cogging. Fig. 7 depicts a photo of a stator segment with its winding.

B. Measured Parameters and No-Load Voltage

Testing such a big generator is rather difficult. However, when a translator segment with permanent magnets was hoisted into the AWS, it moved along the stator and there was an opportunity to measure the no-load voltage. Fig. 8 gives the no-load voltage of a generator part at very low and not exactly constant speed (a few centimeters per second) resulting in a low voltage. Before $t = 40$ s, the overlap between stator and translator is constant. Around $t = 45$ s, there is a stop. After $t = 50$ s, the overlap between stator and translator reduces, resulting in a decreasing no-load voltage while the frequency and the speed remain more or less constant.

By integrating the no-load voltage, the flux linkage was obtained. Fig. 8 also depicts this flux linkage. This flux linkage appears to be sinusoidal, mainly due to the magnet skewing. As

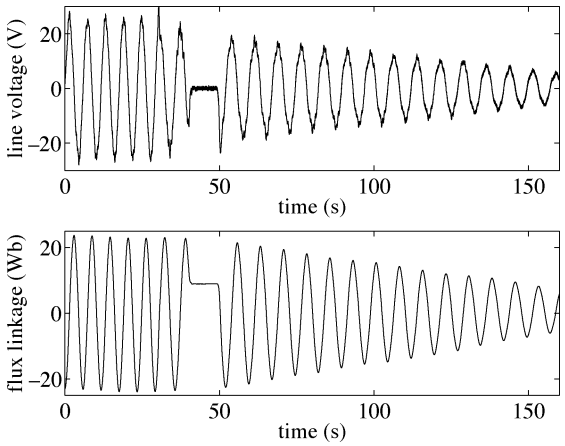

Fig. 8. Measured no-load line voltage and flux linkage of a part of the generator.

TABLE II
COMPARISON OF MEASUREMENTS AND CALCULATIONS

	calculated	measured
flux linkage $\hat{\lambda}_{pm}$	23 Wb	23.5 Wb
leakage inductance L	28 mH	31 mH
resistance R	0.27 Ω	0.29 Ω

in Table II, the value of the flux linkage at complete overlap correlates well with the calculated flux linkage.

The resistance and leakage inductance of the generator were determined by measuring the current response to a step voltage. Also here, the correlation between measurement and calculation given in Table II is reasonable.

C. Performance

Fig. 9 illustrates the operation of the AWS for a typical wave during half a wave period. Position and speed are assumed to vary sinusoidally. Therefore, the amplitude and the frequency of the induced voltage vary continuously. Because of the partial overlap, the rms value of the voltage is not exactly proportional to the speed.

The required force is proportional to the speed. To make this force, the amplitude of the stator currents is controlled by the converter. Here, it is assumed that this current is sinusoidal and in phase with the no-load voltage, which can be realized using a VSI. Although the required force varies sinusoidally, the rms value of the current does not vary sinusoidally: when the overlap reduces, the current has to increase to obtain the required force. This explains the strange form of the rms value of the current.

The losses in the converter are assumed to be 2.5% of the rated power at full load, 0.5% of the rated power in no-load, and 2% proportional to the actual power delivered by the converter. At low power, the converter losses limit the system efficiency considerably. At high power, the cable losses and the copper losses form the most important part of the losses.

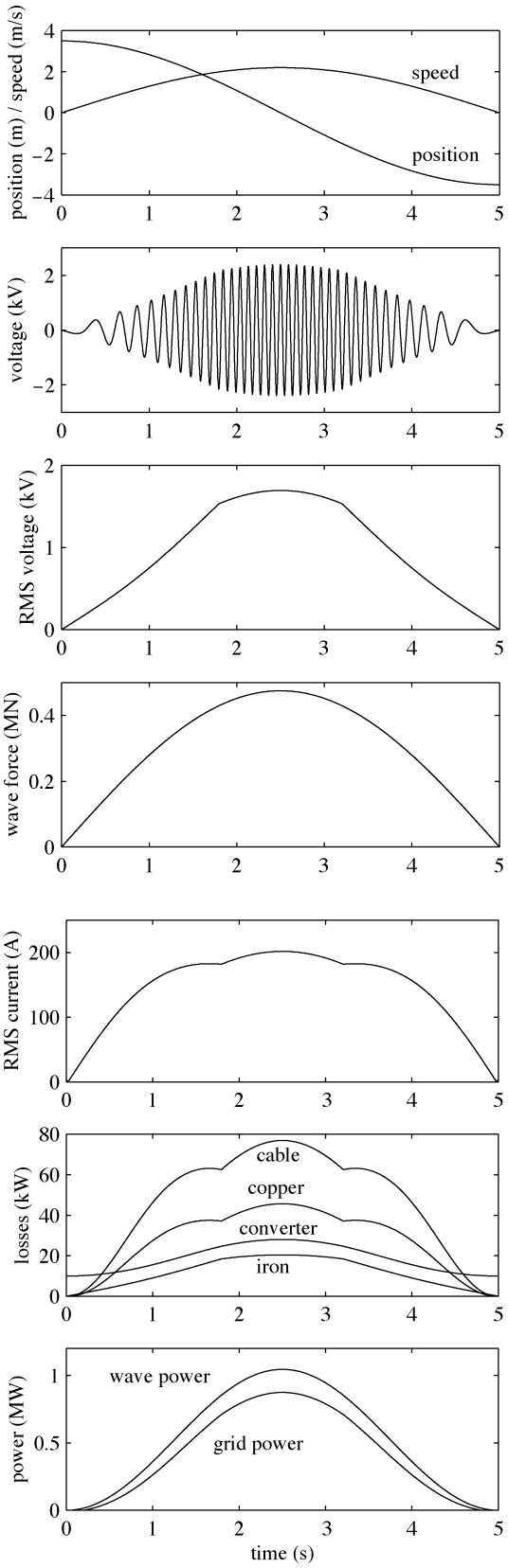

Fig. 9. Position, speed, no-load phase voltage, rms no-load phase voltage, generated force, rms current, losses, and powers as a function of time during half a wave period.

The grid power varies as a squared sinus, which may be a problem when the AWS is connected to a weak grid. The total power of a number of sensibly located AWS systems is probably much more constant.

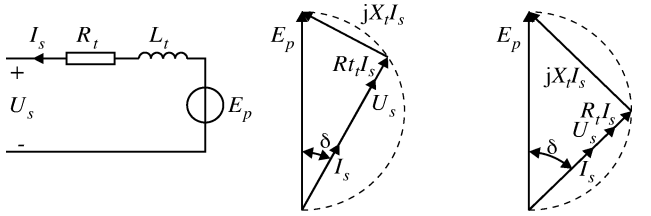

Fig. 10. Equivalent circuit of the PMLSM and the phasor diagram with CSI.

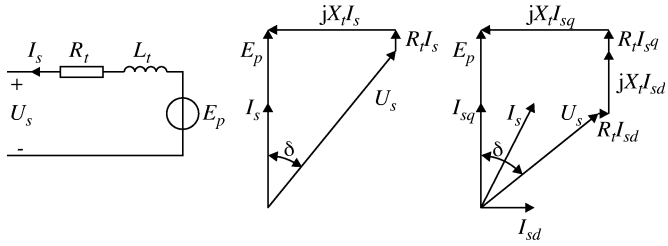

Fig. 11. Equivalent circuit of the PMLSM and the phasor diagram with a VSI.

IV. Converter Choice

As stated earlier, a CSI is used for the grid connection of the AWS pilot plant. Compared to a VSI, the CSI has the following advantages:

- it does not need accurate translator position information;
- it is probably cheaper;
- it is probably more efficient than the VSI because the CSI has lower conduction losses and lower switching losses.

The CSI was chosen mainly because of the first advantage: it is rather expensive and time-consuming to develop a sufficiently accurate position sensor system for the on shore converter.

However, a back-to-back VSI also has important advantages compared to the CSI:

- the power factor at the grid side can be controlled;
- the grid currents can be made sinusoidal;
- the generator force can be larger;
- the generator power factor can be controlled to minimize the generator and cable losses;
- the generator currents can be made sinusoidal.

In this section, the generated force and the annual energy yield of the CSI and the VSI system are compared to decide which inverter should be used in future versions of the AWS.

To make a fair comparison, the maximum line voltage is chosen to be 3000 V and the maximum current is chosen to be 400 A. Further, the voltages and currents are assumed to be sinusoidal.

The generator side of the CSI is a diode bridge rectifier. This diode bridge rectifier is modeled as a resistive load, resulting in the first phasor diagram of Fig. 10. The maximum force with a resistive load is made when the current lags the no-load voltage with 45°, as depicted in the second phasor diagram of Fig. 10.

For the VSI system, the current is kept in phase with the no-load voltage to minimize the copper losses, as indicated in the first phasor diagram of Fig. 11.

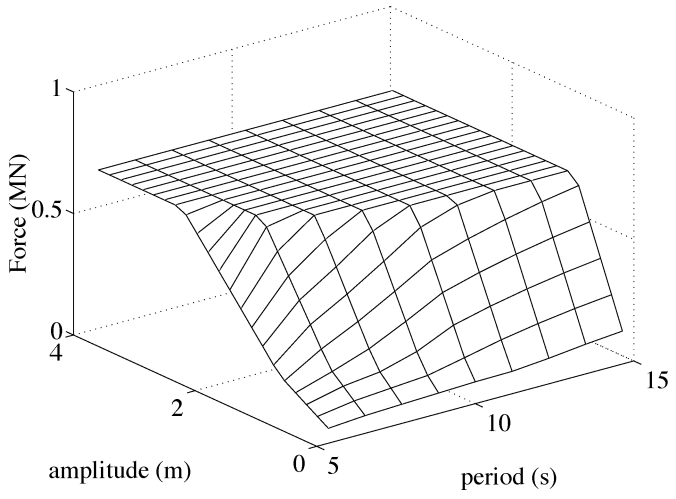

Fig. 12. Generated force as a function of wave amplitude and wave period for the CSI system.

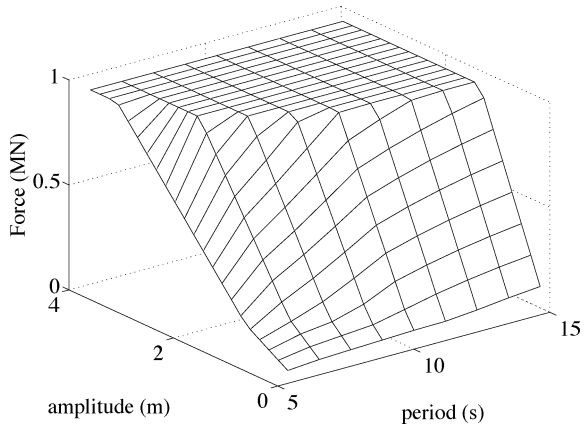

Fig. 13. Generated force as a function of wave amplitude and wave period for the VSI system.

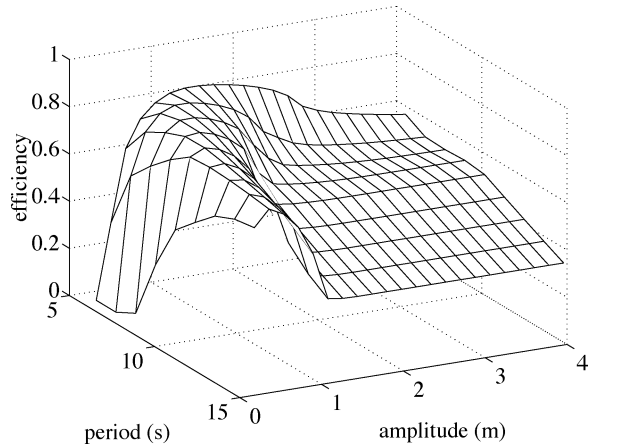

Fig. 14. System efficiency averaged over a wave period as a function of wave amplitude and wave period for the CSI system.

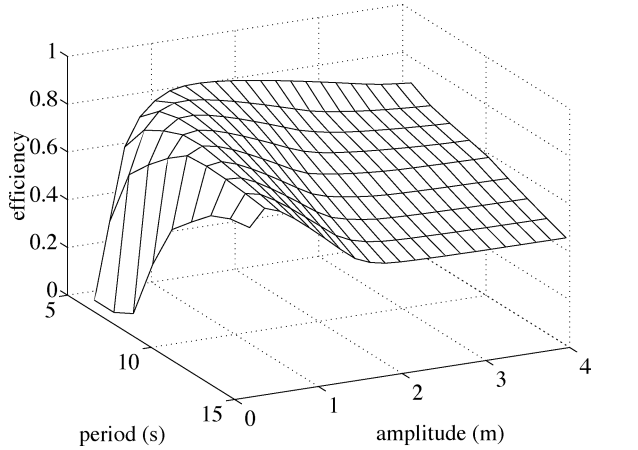

Fig. 15. System efficiency averaged over a wave period as a function of wave amplitude and wave period for the VSI system.

If this results in a terminal voltage higher than the rated voltage, a negative d-axis component of the current is added to limit the voltage to the rated voltage as indicated in the second phasor diagram of Fig. 11.

Figs. 12 and 13 depict the generator force for the CSI system and the VSI system as a function of wave amplitude and wave period. In the CSI system, the current is limited to 400 A, because at this current the maximum power is extracted according to the second phasor diagram of Fig. 10. The maximum force is 659 kN. In the VSI system, the current is also limited to 400 A, which limits the force to 933 kN.

Fig. 14 and Fig. 15 depict the system efficiency for the CSI system and the VSI system respectively. The efficiency is here defined as the electrical energy supplied to the grid divided by the mechanical energy taken by to the generator. The efficiencies are not very high. The VSI system is better, mainly at larger forces, because of the better power factor.

The calculated annual energy output to the grid for the CSI system is 1.64 GWh. Increasing the CSI current rating does not increase the energy yield, because at 400 A, the maximum power is extracted. Adding capacitors could help to increase the energy yield. The calculated annual energy output to the grid for the VSI system is 1.94 GWh. Compared to the CSI system, this is an increase of about 18%, which is substantial. This increase in energy yield is caused by the combination of the higher force and the higher efficiency. Increasing the VSI current rating hardly increases the annual energy yield, although it increases in the generated force. It can be concluded that there are important reasons to use a VSI in future versions of the AWS.

V. Conclusions

This paper describes the generator system of the AWS, which consists of a permanent-magnet linear synchronous generator and a CSI. The PMLSM has been designed and built and the correlation between measured and calculated generator parameters is reasonable. The paper describes a method to calculate the annual energy yield from the wave distribution. For the pilot plant, it is calculated as 1.64 GWh. Using a VSI instead of a CSI improves the power factor, the current waveforms, the efficiency and the generator force, so that the annual energy yield increases with 18%.

References

[1] Ove Arup & Partners, *Wave Energy: Technology Transfer & R&D Recommendations*, London, U.K., 2000.

[2] N. I. Meyer and K. Nielsen, "The Danish wave energy programme second year status," in *Proc. 4th Wave Energy Conf.*, Aalborg, 2000, pp. 10–18.
[3] T. W. Thorpe, "The wave energy programme in the UK and the European wave energy network," in *Proc. 4th Wave Energy Conf.*, Aalborg, The Netherlands, 2000, pp. 19–27.
[4] ——, "A Review of Wave Energy," ETSU Report, R-72, 1992.
[5] ——, "An overview of wave energy technologies, status, performance and cost," in *Dig. Seminar Wave Power, Moving to Commercial Viability*, London, U.K., 1999.
[6] S. S. Y. Narayanan, B. K. Murthy, and G. S. Rao, "Dynamic analysis of a grid-connected induction generator driven by a wave-energy turbine through hunting networks," *IEEE Trans. Energy Conversion*, vol. 14, pp. 115–121, Mar. 1999.
[7] M. A. Mueller, "Electrical generators for direct drive wave energy converters," in *Proc. Inst. Elect. Eng. Generation, Transmission and Distribution*, vol. 149, 2002, pp. 446–456.
[8] L. W. M. M. Rademakers, R. G. Van Schie, R. Schuitema, B. Vriesema, and F. Gardner, "Physical model testing for characterising the AWS," in *Proc. European Wave Energy Conf.*, Patras, Greece, 1998.
[9] A. J. N. A. Sarmento, A. M. Luíd, and D. B. S. Lopes, "Frequency-domain analysis of the AWS device," in *Proc. European Wave Energy Conf.*, Patras, Greece, 1998.
[10] H. Polinder, F. Gardner, and B. Vriesema, "Linear PM generator for wave energy conversion in the AWS," in *Proc. 8th Int. Conf. Electrical Machines*, Helsinki, Finland, 2000, pp. 309–313.
[11] T. Sebastian and G. R. Slemon, "Transient torque and short-circuit capabilities of variable speed permanent magnet motors," *IEEE Trans. Magnetics*, vol. MAG-23, pp. 3619–3621, 1987.
[12] H. Polinder, M. E. C. Damen, and F. Gardner, "Modeling and test results of the AWS linear PM generator system," in *Proc. 9th Int. Conf. Electrical Machines*, Brugge, Belgium, 2002.
[13] D. Patterson, A. Monti, C. Brice, R. Dougal, R. Pettus, D. Srinivas, K. Dilipchandra, and T. Bertoncelli, "Design and simulation of an electromagnetic aircraft launch system," in *Proc. 37th Industry Applications Ann. Meeting*, vol. 3, Pittsburgh, 2002, pp. 1950–1957.
[14] R. Richter, *Elektrische Maschinen, erster Band*, 3rd ed. Basel: Birkhäuser, 1967.

Henk Polinder (M'97) was born in Nunspeet, The Netherlands, in 1968. He received the M.Sc. and Ph.D. degrees from Delft University of Technology, Delft, The Netherlands, in 1992 and 1998 respectively.

Since 1996, he has been an Assistant Professor in the Electrical Power Processing Group of Delft University of Technology. He is mainly interested in design aspects of electrical machines for renewable energy and mechatronic applications.

Michiel E. C. Damen was born in The Hague, The Netherlands, in 1976. He received the B.Sc degree from the Technical Highschool Rijswijk, Rijswijk, The Netherlands, in 1998, and the M.Sc. degree from Delft University of Technology, Delft, The Netherlands, in 2003.

Currently he is with Teamwork Technology BV, Zijdewind, The Netherlands. He is also with the Technical Highschool Rijswijk. His main research interests are electrical power aspects of renewable energy sources.

Fred Gardner was born in Brisbane, Australia, in 1956, and immigrated to The Netherlands in 1963. He is educated as engineer in mechanics and electrics and teaching.

Since 1993, he has been Director of Engineering of Teamwork Technology BV, Zijdewind, The Netherlands, where he is responsible for concept engineering and product development of products such as the Archimedes Wave Swing. His special interest is the management of the innovation process.